

Three-dimensional distribution of fine particulate matter concentrations and synchronous meteorological data measured by an unmanned aerial vehicle (UAV)

Si-Jia Lu¹, Dongsheng Wang¹, Xiao-Bing Li¹, Zhanyong Wang¹, Ya Gao¹, Zhong-Ren Peng^{1,2}

¹ Center for UAV Application and ITS Research, State Key Laboratory of Ocean Engineering, School of Naval Architecture, Ocean & Civil Engineering, Shanghai Jiao Tong University, Shanghai, 200240, China

² Department of Urban and Regional Planning, University of Florida, Gainesville, FL 32611-5706, USA

Correspondence to: Z. R. Peng (zpeng@dcp.ufl.edu)

Abstract. Three-dimensional distribution of fine particulate matter ($PM_{2.5}$) and meteorological factors are of great importance for clarifying the formation mechanism of haze pollution and developing atmosphere pollution forecasting model. The objective of this study is to measure $PM_{2.5}$ concentrations and synchronous meteorological data at 300-1000 m altitude using an unmanned aerial vehicle (UAV) equipped with mobile instruments. The experiments were conducted for five days from 21th August 2014 to 2nd February 2015, in a $4 \times 4 \text{ km}^2$ space in Lin'an, China. The UAV was operated repeatedly along the designed spiral route up to 1000 m altitude four times a day in order to study spatial distribution of $PM_{2.5}$ concentrations and its diurnal variations. Air temperature, relative humidity, dew point temperature, pressure and GPS were also sampled along the flight. The study indicates that the vertical distribution of $PM_{2.5}$ concentrations presents obvious stratification in morning flights compared with that in afternoon flights. The horizontal distribution of $PM_{2.5}$ concentrations appears more homogeneous than vertical distribution on experiment days. $PM_{2.5}$ concentration levels over 500 m height in afternoon flights are generally higher than those of morning flights (except for on February 5th, 2015). This indicates that the planetary boundary layer (PBL) height and inversion layers have a significant impact on the near ground $PM_{2.5}$ concentration. $PM_{2.5}$ concentrations are positively correlated with dew point temperature, which likely reflects the compound aerosol-cloud interactions. These findings are crucial for correcting $PM_{2.5}$ pollution forecast and environmental management.

1 INTRODUCTION

Ambient air pollution is a primary environmental problem in industrial and developing countries, and China has not been spared (Ouyang et al., 2013). Fine particulate matter holds the key to some of the greatest mysteries of climate science (Davidson et al., 2005; Booth et al., 2012; Stevens et al., 2012) The complex interactions between aerosol particles and climate are reported and different components of particulate matter can have either warming or cooling effects on the climate (available at: <https://www.epa.gov/air-research/air-quality-and-climate-change-research>, 2016). Fine particulate matter also threatens human health, especially the cardio-respiratory system (Pope et al., 2002, 2009; Dominici et al., 2006).

Vertical profiles of fine particulate matter concentrations and meteorological data are vital for investigating the formation and dispersion mechanisms of fine particulate matter pollution. Understanding the mechanisms is in turn significant for air pollution forecasts and urban planning. However, most of the previous studies focused mainly on the characteristics of fine particulate matter at a surface level. Most of the previous studies mainly focused on the characteristics of fine particulate matter at a surface level. Solely ground-based observations are insufficient for a correct understanding of the trans-boundary transport of pollutants (Ding et al., 2009), and of the influence of atmospheric microcirculation (e.g. sea-land breeze, urban heat island effect) on pollutant distribution in urban areas (Strawbridge et al., 2004). Also, climate models are based on simplifications that ignore the complexity of the small scale physical processes. It is necessary to calibrate climate models with detailed and parameterised measurement data (Boy et al., 2006; Ding et al., 2009).

Techniques, e.g., meteorological tower, tethered balloons, LiDARs, manned aerial vehicles and unmanned aerial vehicles, are routinely utilised in measuring particulate matter vertical profiles in the troposphere and planetary boundary layer (PBL). A meteorological tower could be used for long-term and continuous observations, but is limited in terms elevation and mobility (Ding et al., 2005; Yang et al., 2005). Compared with a meteorological tower, a tethered balloon could extend the monitoring scale to a higher atmosphere (over 350 m) (Li et al., 2015; Renard et al., 2016). Also, PM concentrations at continuous height levels could be obtained with a tethered balloon. Nevertheless, it is restricted to a horizontal monitoring range. LiDAR is a simple and efficient method of monitoring PM concentrations indirectly, but the accuracy of the measurement remains questionable. Manned aerial vehicles can undertake a large range of measurements, but could not be used extensively due to the high cost of operation (Wang et al., 2008).

Fine particulate matter makes up the dominant fraction of particulate matter in the troposphere (Wang et al., 2008). Generally, PM_{2.5} concentrations logarithmically decrease with increasing altitude and the vertical distributions are classified into two patterns: gradual decline pattern and rapid decline pattern (Ding et al., 2005; Yang et al., 2005). However, the PM_{2.5} concentration distributions could be affected by multiple factors, e.g., meteorological factors, PBL structure and the changing of the wind (Strawbridge et al., 2004; Wang et al., 2008; Sun et al., 2013). Fine particulate matter tends to be well mixed vertically during daytime (Maletto et al., 2003), while layers of fine particulate matter are discovered in wintertime nocturnal settings (Mckendry et al., 2004). The reverse distribution of relative humidity (RH) might explain the “higher-top and lower-bottom” pattern of the PM_{2.5} distributions, considering the moisture absorption (Sun et al., 2013).

Use and development of unmanned aerial vehicle (UAV) technology has risen in recent years. Although restricted by the battery endurance and limited maximum payload, UAVs have been applied in multiple industries, e.g., surveying and mapping, precision agriculture and construction. Considering the cost, performance and manoeuvrability in comparison with manned aircraft, UAVs, both fix-wing UAVs and quadrotors, have been recently utilised for measuring meteorological factors (Kroonenberg et al., 2008; Wildmann et al., 2013; Wildmann et al., 2014; Altstätter et al., 2015), atmosphere structure (Thomas et al., 2012; Wildmann et al., 2014; Lathon et al., 2014) and particulate matter (Clarke et al., 2002; Harnisch et al., 2009; Bates et al., 2013; Altstätter et al., 2015; Brady et al., 2016). An asymmetry in the aerosol distribution was discovered in the cross-valley direction which could be explained by differences in orientation and albedo of the two

valley slopes (Harnisch et al., 2009). Frequent aerosol layers were found aloft with high PNC and enhanced aerosol light absorption (Bates et al., 2013). A particle burst event was obtained during the boundary layer development in the morning (Altstädter et al., 2015). PM₁₀ and PM_{2.5} were influenced by similar sources over PRD, China, and the average ratio of PM_{2.5} to PM₁₀ was 0.84 (Wang et al., 2008). In summary, most research has been focused on the vertical distributions of PM concentrations, but few study the three-dimensional distribution of fine particulate matter, especially during the formation and dispersion events.

In this article, the UAV research was undertaken to investigate 3D distribution of PM_{2.5} concentrations and to explore the relationship of the diurnal variations of spatial distribution with meteorology. A total of 20 monitoring flights in three seasons were carried out over the suburban area of Lin'an, China. In Sect. 2, the experiments site, experimental program and data processing methods are introduced. In Sect. 3, the diurnal variations of PM_{2.5} concentrations as well as the PM accumulation and dispersion events are discussed in detail. Finally, a summary of this article and a conclusion of 3D measurements are provided in Sect. 4.

2 EXPERIMENTS AND METHODS

2.1 Experimental Site

Mobile 3D measurements were performed in a 4 × 4 km² suburban area in the northern part of Lin'an, China (29°56'-30°23'N, 118°51'-119°52'E) (see Figure 1). Lin'an has a subtropical monsoon type climate with four quite distinct seasons and north eastern winds prevail in winter, whilst southerly winds reign in summer (Meng et al., 2012; Peng et al., 2015). The experimental site is approximately 13 km distant from the downtown. The Changxi Provincial Highway runs alongside the Zhongtiaoxi River west-to-east across the experiment site. A hi-tech development zone located on the southern side of the highway is under construction. Thirteen machinery manufacture plants are operated in the hi-tech zone. Some residential areas are located on the northern side of the highway. No direct pollution sources are within or close to the experiment site. Less than 10% of the experiment site is residential land surrounded only by hills on the southeast and northwest of the area. In the experiment site, nearly half of the ground is covered by trees and one-third of the surface is bare land.



Figure 1. The location and the satellite aerial photography of the experiment site in Lin'an, China.

2.2 Mobile Monitoring

- 5 Mobile 3D measurements were performed with an UAV equipped with fast-response instruments for measuring $PM_{2.5}$ concentrations and meteorology in the lower troposphere, especially within the PBL. (see Figure 2). This fixed-wing UAV was modified from an air-mapping aircraft manufactured by the Second Surveying and Mapping Institute of Zhejiang Province. It has a wingspan of 2.4 m, a maximum take-off weight of about 15 kg and a maximum payload of 5 kg. The UAV is powered by a gasoline engine with a maximum output power of 2800 kW. The engine is at the front of the UAV and the exhaust fumes are released is above the nose of the UAV. Safe operation is possible at a wind speed of 12 m s^{-1} . The cruising speed is typically $30\text{ to }35\text{ m s}^{-1}$. $2 \times 1.5\text{ L}$ tanks allow flight endurance for over one hour. The UAV was controlled by a pilot when it took off and landed. When it reached 300 meters high, the operator switched over to autopilot. The UAV climbed in a spiralling fashion from 300 m to more than 1000 m altitude along the designed route at the speed about 30 m s^{-1} . Specifically, the UAV climbed 50 m after finishing one rectangle and continued on to the next one. Considering the time resolution of the measurements (see Table 1), one flight would last for about 30-40 minutes so that it was possible to collect enough data at each vertical altitude level.

带格式的：字体：10 磅，非加粗



Figure 2. Left picture shows the UAV and instruments arrangement. The gasoline engine (1) is mounted at the tip of the aircraft. The GPS receiver (2) is positioned outside. PM detector and BC measurer are installed the middle compartment (3) of the plane.

The temperature/relative humidity probe (4) and all inlets (5) are positioned under the plane underside. Right picture shows the flight route and 3D terrain landscape with Google Earth.

The onboard portable instruments all are listed in Table 1. PM_{2.5} concentrations were measured by a Sidepak Personal Aerosol Monitor AM510 (TSI, Inc.). As presented in our previous studies (Wang et al., 2015a, b), the PM monitor was calibrated before leaving factory and further estimated with standard methods at outdoor locations in Shanghai, China, prior to this field study. A comparison experiment was undertaken between the PM monitor and TEOM mass measurement devices at Shanghai Environmental Monitoring Centre. The comparison experiment lasted for 21 days and was conducted under different temperature and humidity conditions. The results show that the data captured by Sidepak AM510 PM Monitor is quite consistent with the TEOM data, with correlation coefficient (R) of 0.99, intercept of -11.52 and slope of 0.82. Air temperature (T), relative humidity (RH) and dew point temperature were measured with a HOBO U12 Temp/RH Data Logger, which was fixed outside the fuselage. Air pressure was measured by a pressure sensor built in a POM Ozone Monitor (2B technology, Inc.). The PM and Ozone monitors were wrapped with a foam buffer to avoid vibration problem. Latitude, longitude and height information was recorded by a Columbus V-900 Multifunction GPS receiver. No measurements for dew point temperature were recorded during flight-2 to 4 on 21th August 2014 due to equipment failures. The logging time of all onboard instruments was strictly synchronized with BST (Beijing Standard Time).

All tubing on the instrument inlets were made of either tygon or conductive-silicon tubing. All the inlets were positioned on the UAV underside which has been testified with the DPM model to be an optimal placement to avoid the turbulence (Zhang et al., 2014). With the build-in sampling pump, air was pumped into a sampling tube through an inlet that towards the UAV tail in order to avoid exhaust pollution and the effect of variation of the flow rate. The length of tubing from the manifold to each instrument was minimized to reduce particle loss due to sorption.

Table 1. Particles and Meteorology Monitoring Equipment on UAV.

Parameter	Equipment	Detection limit	Instrument reporting interval (s)
PM _{2.5}	Sidepak Personal Aerosol Monitor AM510 (TSI, Inc.)	0.001 mg m ⁻³	2
Air temperature	HOBO Temperature and Relative Humidity Probe	0.03 °C	2
Relative humidity		0.03 %	
Dew point		0.03 °C	
Pressure	Pressure sensor built in POM Ozone Monitor (2B Technology, Inc.)	0.1 Torr	10
Latitude	Columbus V-900 Multifunction GPS Data Logger		1
Longitude			
Height			

3D measurements were taken for five days on August 21th (in summer), October 11th, November 14th (in autumn), December 12th in 2014 and February 5th in 2015 (in winter). Four flights were done on each experiment day, equalling a total of 16 flights. The detailed information about flight schedules, weather conditions and meteorology factors were provided in Table 2. These data was downloaded from the Air Quality On-line Monitoring and Analysis Platform of China (<http://www.openair-project.org/Examples/WindPollutionRoses.aspx>, last access: 2nd March 2015), maintained by Lin'an regional background station (30°18' N, 119°44' E). The flights executed after sunrise, before noon, after noon and before dusk were named as flight-1, flight-2, flight-3 and flight-4, respectively. Effective sampling time during a flight was generally 25-30 minutes.

Table 2. Flight Schedules and Meteorology during Measuring Flights.

Date	Effective flight time(BST)	Weather conditions	PM _{2.5} ($\mu\text{g m}^{-3}$)	Temperature (°C)	Humidity (%)	Wind direction (hr)/ Wind Scale
2014-8-21	6:26-7:00	Cloudy	25	20	99	SW/2
	10:17-10:52	Cloudy	23	25	78	SE/1
	14:11-14:46	Cloudy	15	30	60	NE/2
	16:22-16:57	Cloudy	16	30	58	E/2
2014-10-11	7:32-8:09	Cloudy	46	21	86	E/2
	10:02-10:39	Cloudy	28	23	63	NE/3
	14:00-14:35	Cloudy	23	26	52	E/3
	15:47-16:22	Cloudy	27	24	57	NE/3
2014-11-14	7:28-8:01	Cloudy	46	3	89	SW/1
	10:02-10:37	Cloudy	48	12	53	SE/1
	14:02-14:37	Cloudy	44	16	34	NE/3
	15:33-16:07	Cloudy	51	15	34	NE/3
2014-12-12	8:08-8:46	Sunny	104	2	87	SE/1
	10:35-11:17	Sunny	95	5	41	N/1
	14:22-15:02	Sunny	37	9	26	W/3
	15:32-16:13	Sunny	33	8	27	W/3
2015-2-5	8:08-8:45	Cloudy	151	0	89	NE/1
	10:44-11:21	Sunny	190	5	51	E/1
	14:14-14:50	Sunny	36	8	31	N/3

Note: GMT = Beijing Standard Time (BST)–8h. Force 1 wind = 0.3-1.5 m s⁻¹; force 2 wind = 1.6-3.3 m s⁻¹; force 3 wind = 3.4-5.4 m s⁻¹.

Before each take-off, the status of instruments, e.g., remaining battery and storage space, were checked, the logging time was all synchronized and a visual inspection was conducted to prevent the possible extrusion of inlet tubings. The PM and Temperature/RH monitors were warmed up for at least 20 min prior to calibration. When the temperature was less than 10°C, the warm-up time would be extended to 35-40 min to ensure stable readings. After the PM monitor had warmed up, the calibrations were checked with 0 µg m⁻³ (Padr6-Mart ńez et al., 2012).

2.2 Data Processing and Analysis

The sampling PM, meteorology and GPS data was exported and aggregated by flight. The data process consists of several steps. First, measurements associated with instrument errors, as noted in the flight log, were removed. The next step was to remove exceptional values that contaminated by the exhaust from the UAV. The PM data could be contaminated during the taking-off and descending periods. Based on the high resolution GPS data recorded by the GPS logger, data sampled below 300 m altitude and during descent stage was excluded (Peng et al., 2015). Third, the outliers judged by 3-sigma principle were excluded. Overall, 18% of the sampling data was removed.

Considering that the Sidepak AM 510 PM monitor is founded on the light scattering principle, the samples PM concentrations can be impacted by relative humidity (Mamouri et al., 2013). Thus, a correction factor (CF) is used to compensate for this error. The results fit the actual data quite well after the correction (Ramachandran, et al., 2003). CF is expressed as follows:

$$CF = 1 + \frac{RH^2}{4(1-RH)} \quad (1)$$

where, RH denotes relative humidity.

After the data cleaning and calibrating, the processed data with different time resolutions was averaged to 10 seconds in order to further eliminate noise and to facilitate data interpretation.

3 RESULTS AND DISCUSSION

3.1 Spatial Distribution of Particle Mass Concentration

The 3D distributions of PM_{2.5} concentrations during 20 flights were mapped in Figure 3. The PM_{2.5} concentrations present a stratification distribution and the horizontal distribution of fine particulate matter at each height level is much more uniform than vertical distribution. This is likely to be no pollution sources on the local scale. The vertical distribution of PM_{2.5} concentrations appears a typical diurnal variation. To further analyse the vertical diurnal variation of PM_{2.5} concentrations and its relationship with the meteorological factors, the 10-second-averaged data was averaged for each height layer.

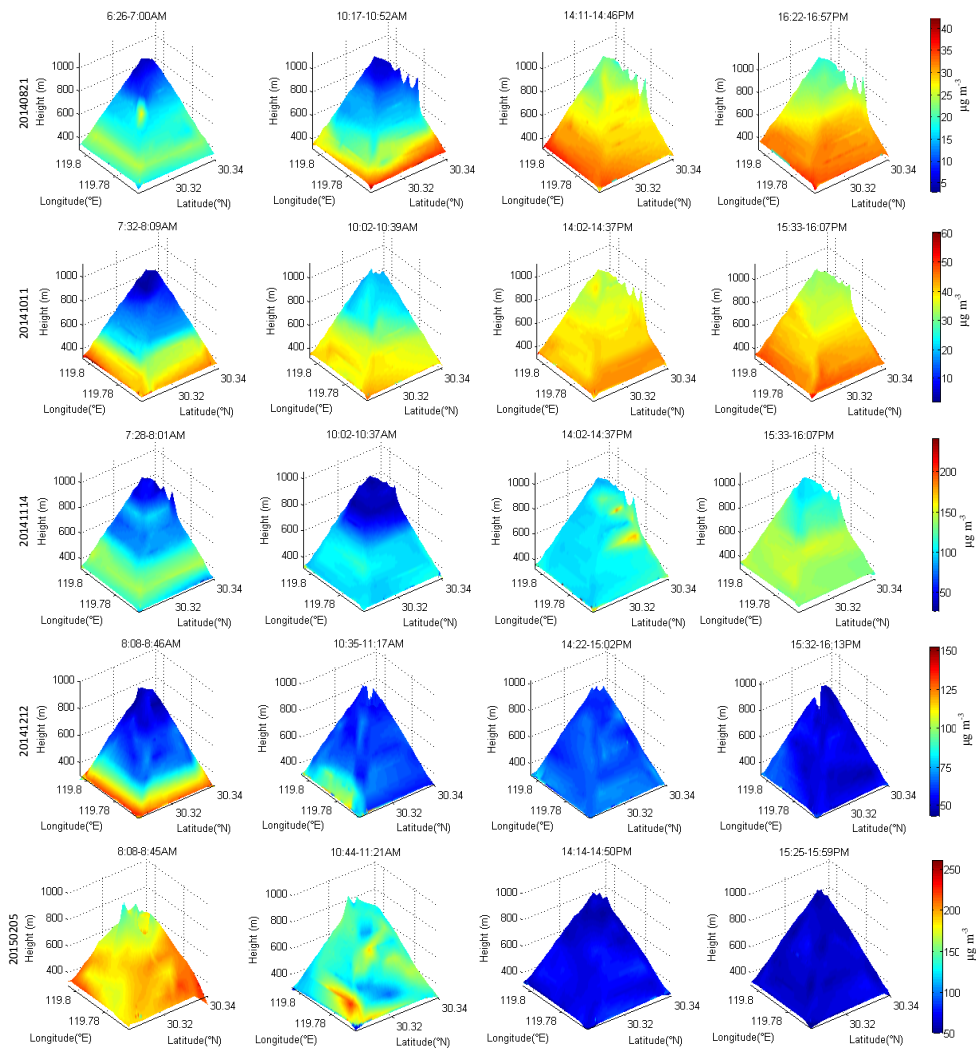


Figure 3. Spatial distribution of PM_{2.5} concentrations.

Vertical profiles of PM_{2.5} concentrations are illustrated in Figure 4. For the sake of simplicity, flight-1 and flight-2 are grouped as morning flights, and flight-3 and flight-4, as afternoon flights in this article. In general, PM_{2.5} concentrations measured during both morning flights and afternoon flights decrease with increasing altitude, which corresponds to a “higher-bottom and lower-top” pattern (Šmidl et al., 2013) and is consistent with results from tower observations (Liao et al., 2014). However, the vertical distribution pattern in morning flights is different from that in afternoon flights (see Figure 4). There is a relatively big difference between 300 m and 1000 m after sunrise (see Figure 4, flight-1). These observations prove that the PBL height has a significant impact on the vertical distribution of PM_{2.5} concentrations. The PBL height is relatively low at night and early morning and it limits PM_{2.5} to transport upward. Atmosphere convection is strengthened as PBL height increases over 1000 m in the late morning. Thus, particulate matter under PBL height is mixed up and vertical distribution of PM_{2.5} concentrations in afternoon flights tends to be homogeneous. Linear regression is conducted to illustrate the vertical variations of PM_{2.5} concentrations (see Table 3). The absolute slope of vertical profiles in morning flights are apparently higher than of those in the afternoon flight (1.68-13 times). The PM_{2.5} concentration average at 300-1000 m altitude in the afternoon is higher than in the morning, likely to reflect the contribution of atmospheric turbulence to the increasing particulate matter concentration in the afternoon. This is consistent with the findings of Ding et al. (2005). On pollution days (2014/11/14, 2014/12/12, and 2015/2/5), the slope of PM_{2.5} concentration vertical profiles ranges from -0.1281 to -0.1020 during flight-1, while it ranges from -0.1381 to -0.0225 during flight-2, from -0.0178 to -0.0076 during flight-3 and from -0.2320 to 0.0011 during flight-4.

带格式的：字体：10 磅，非加粗

带格式的：字体：10 磅，非加粗

带格式的：字体：10 磅，非加粗

带格式的：字体：10 磅，非加粗

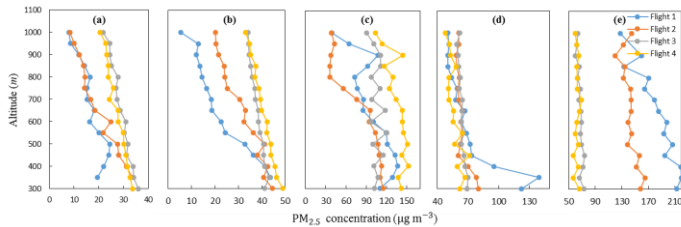


Figure 4. Vertical profiles of PM_{2.5} mass concentration during all flights. Flights 1-4 are marked with blue, red, grey and yellow lines, respectively. (a) 2014/8/20; (b) 2014/10/11; (c) 2014/11/14; (d) 2014/12/12; (e) 2015/2/5.

Table 3. The Slope of the Vertical Profiles of PM_{2.5} Concentrations.

	Flight-1	Flight-2	Flight-3	Flight-4
2014/8/21	-0.0220	-0.0382	-0.0178	-0.0180
2014/10/11	-0.0541	-0.0379	-0.0128	-0.0206
2014/11/14	-0.1027	-0.1381	-0.0076	-0.0478
2014/12/12	-0.1020	-0.0225	-0.0127	-0.2320

2015/2/5	-0.1281	-0.0397	-0.0140	0.0011
----------	---------	---------	---------	--------

3.2 Meteorological Factors

The vertical profiles of air temperature, dew point temperature, and relative humidity at 300-1000 m are illustrated in Figure 5 where the UAV and sounding data is marked with solid and dashed lines respectively. Sounding meteorological data (including air temperature, dew point temperature, relative humidity, wind speed and wind direction) were sampled at the sounding station located in Hangzhou (Station identifier: ZSHC; Station number: 58457; 30°13' N, 120°10' E), about 40 km away from the experiment site. The sounding are operated twice a day (at UTC 0:00 and 12:00 everyday) and the sampling dataset can be downloaded from the website of University of Wyoming (available at: <http://weather.uwyo.edu/upperair/sounding.html>, 2016). The sounding data sampled at BST 8:00am is comparable with the UAV data during flight-1. For air temperature, the dashed lines are between the UAV vertical profiles, indicating that UAV air temperature data is in agreement with the sounding ones. For dew point temperature and RH, although the UAV data are not compared well with sounding data, the trend of sounding data is consistent with the data of flight-2 (shown by the orange lines). This difference could be explained by time lag considering the spatial distance and land use difference between the two sampling sites. Compared with sounding data, the UAV data could not only characterise the 3D distribution of meteorological data, but also provide more precise data for further quantitative analysis.

带格式的：字体：10 磅，非加粗

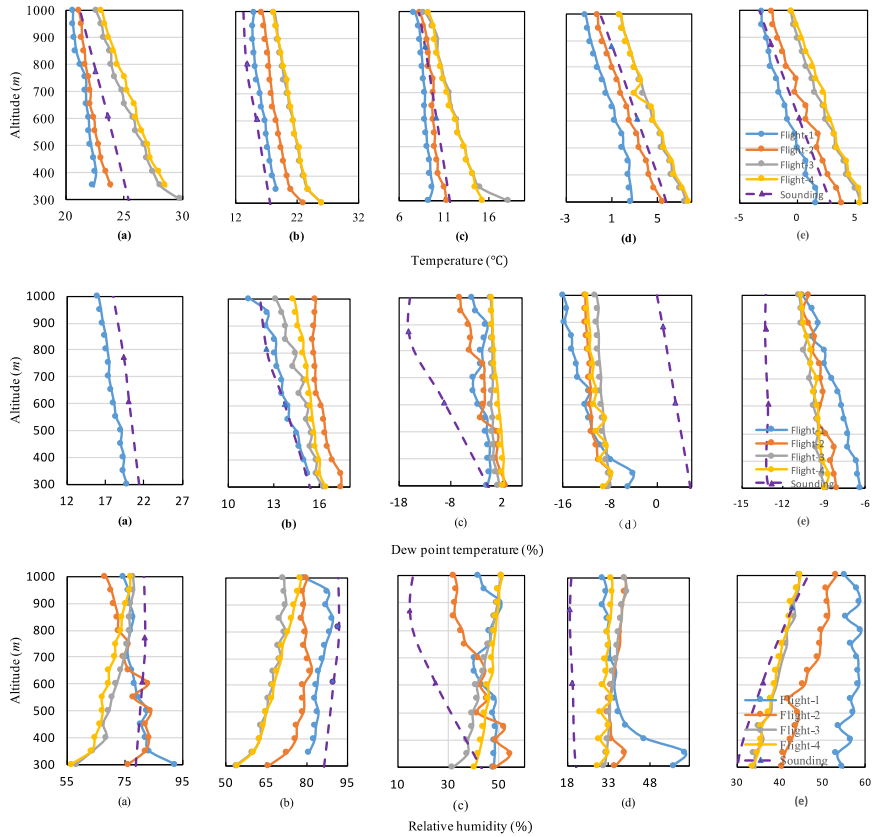


Figure 59. Vertical profiles of air temperature, dew point temperature and relative humidity measured by UAV (solid lines) and by sounding (dashed lines). (a) 2014/8/20; (b) 2014/10/11; (c) 2014/11/14; (d) 2014/12/12; (e) 2015/2/5.

5

To study the relationships among $PM_{2.5}$ concentrations and meteorological parameters, the [normality test has been conducted in our previous work \(Peng et al., 2015\)](#). Amongst them, Pearson's correlations were calculated on the basis of the mean values of each [height layer](#) from 300 m to 1000 m. The obtained correlation coefficients are given in [Table 4](#), together with their significance levels.

Table 4. Pearson's Correlation Coefficients among PM_{2.5} Concentrations and Meteorological Parameters.

		PM _{2.5}	Temp	RH	Dewpoint	Pressure
2014/8/21	PM _{2.5}	1	0.313**	-0.142**	0.032	0.750**
	Temp		1	-0.800**	-0.852**	0.140**
	RH			1	0.632**	-0.018
	Dewpoint				1	.223
	Pressure					1
2014/10/11	PM _{2.5}	1	0.761**	-0.666**	0.857**	0.583**
	Temp		1	-0.916**	0.742**	0.477**
	RH			1	-0.531**	-0.259**
	Dewpoint				1	0.797**
	Pressure					1
2014/11/14	PM _{2.5}	1	0.447**	0.319**	0.690**	0.497**
	Temp		1	-0.338**	0.664**	0.467**
	RH			1	0.477**	0.037
	Dewpoint				1	0.614**
	Pressure					1
2014/12/12	PM _{2.5}	1	-0.011	0.854**	0.764**	0.502**
	Temp		1	-0.364**	0.528**	0.686**
	RH			1	0.591**	0.147**
	Dewpoint				1	0.710
	Pressure					1
<u>2015/2/5</u>	PM _{2.5}	1	0.010	-0.001	0.068*	0.034
	Temp		1	-0.840**	0.005	0.833**
	RH			1	0.532**	-0.423**
	Dewpoint				1	0.513**
	Pressure					1

** Correlation is significant at the 0.01 level (one-tailed); * correlation is significant at 0.05 level (one-tailed).

- 5 From Table 4, the PM_{2.5} concentrations positively correlate with the dew point. This indicates that the vertical distribution of dew point temperature has a strikingly positive impact upon the distribution of PM_{2.5}. Notably, PM_{2.5} concentrations negatively correlate with relative humidity on clean days (21 August and 11 October), but positively correlate on pollution

days. This is likely to reflect the compound aerosol-cloud interactions (Booth et al., 2012; Stevens et al., 2012), since exceptionally high relative humidity could be a key inducing factor for particle formation and accumulation due to its hygroscopicity (Ding et al., 2005; Quan et al., 2011; Bates et al., 2013). The correlations of the PM_{2.5} concentrations with temperature and pressure remain uncertain.

5 3.3 Accumulation Event for PM_{2.5} (2014/11/14)

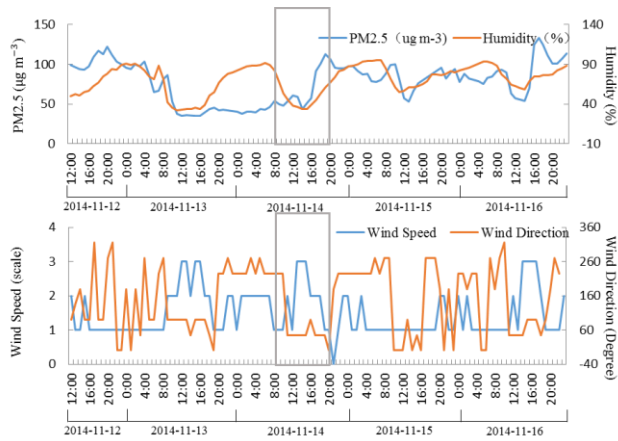


Figure 6. Surface PM_{2.5} concentrations, relative humidity, wind speed and wind direction measured by Lin'an regional background station (30°18' N, 119°44' E) on 12th-16th November. The period of experiment is marked by grey box line.

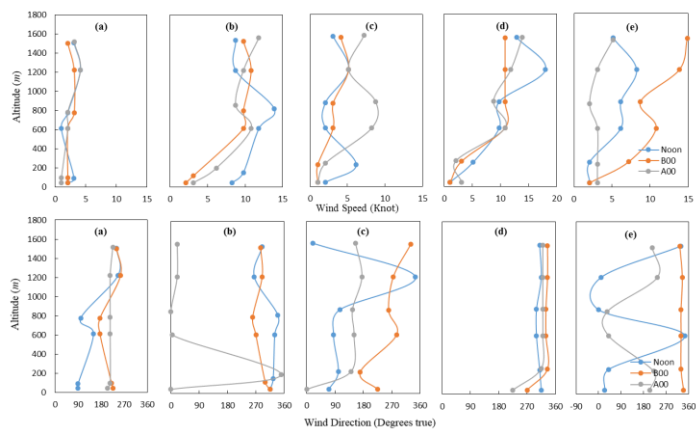


Figure 7. Wind speed and wind direction in 0-1800 m altitude by sounding, (a) 2014/8/21; (b) 2014/10/11; (c) 2014/11/14; (d) 2014/12/12; (e) 2015/2/5. The sounding data marked with grey lines was sampled at BST 8:00am on the experiment day.

- 5 [Figure 6](#) shows a time series of hourly averaged $PM_{2.5}$ concentrations and relative humidity at ground level from 12th to 16th November 2014. Fine particulate matter accumulated from 14:00 on 14th November and climbed to peak value of $\sim 113 \mu g m^{-3}$ at 19:00 on 14th November. The 14th November was a day that provided static weather condition (see [Figure 5 \(c\)](#)). Wind speed at 0-1500 m altitude was no more than 5 knots which was unfavourable for air pollutants to disperse horizontally and the wind blew from the east below 900 m and from the north above 900 m. Our monitoring campaign was operated
- 10 during the pollution accumulation stage, starting from BST 7:30 to 16:00, including four flights. During flight-1 (BST 7:28-8:01), $PM_{2.5}$ concentrations exhibited a positive vertical gradient at 300-400 m and 800-900 m altitude. Meanwhile, Dew point temperature also displayed a positive vertical gradient at 300-400 m and 700-900 m (see [Figure 5 \(c\)](#)). This suggests that shallow thermal inversion layers developed at these two altitude layers, leading to the steady atmospheric stratification and plenty of moisture. Therefore, fine particulate matter was trapped in the thermal inversion layer (Platis et al., 2015).
- 15 During flight-2 (BST 10:02-10:37), the vertical gradient of $PM_{2.5}$ concentrations turned to negative (about -0.054) below 650 m, but sharply increased to -0.399 at 650-800 m. This could be explained by the dilution effect of the weak clean air from the north (see [Figure 5](#)). The average level of $PM_{2.5}$ concentrations at 300-1000 m altitude increased from $98 \mu g m^{-3}$ during flight-1 to $134 \mu g m^{-3}$ during flight-4 (BST 15:33-16:37). This is because air humidity increases apparently with the wind direction changing from north to west, which accelerates the coagulation of particulate matter.

带格式的：字体：10 磅，非加粗

带格式的：字体：10 磅，非加粗

带格式的：字体：10 磅，非加粗

3.4 Dispersion Event for PM_{2.5} (2014/12/12 and 2015/02/05)

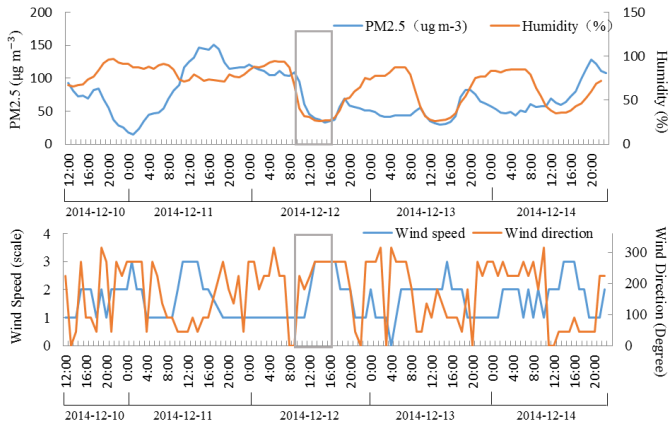


Figure 8. Surface PM_{2.5} concentration, relative humidity, wind speed and wind direction measured by Lin'an regional background station (30°18' N, 119°44' E) on 10th -14th December. The experiment period is marked by grey box line.

Figure 8 shows that the sampling campaign on 12th December captured a dispersion process of PM_{2.5}. Particle matter accumulated at BST 0:00 on 11th December, lasting about nine hours and began to dilute at BST 9:00 on 12th December. At about BST 15:00 on 12th December, PM_{2.5} concentrations dropped to the minimum at 33 μg m⁻³. PM_{2.5} concentrations exhibited a positive vertical gradient at 300-350 m altitude during flight-1. This phenomenon can be explained by the shallow thermal inversion layer at 300-350 m (see Figure 5 (d)). It can be seen from Figure 7(e) that the wind direction remained unchanged but the wind speed increased with altitude during the sampling campaign (Li et al., 2015). As a whole, this presented a typical pollution event caused by regional horizontal transport, and a dispersion process resulted from the foreign clean air.

带格式的：字体：10 磅，非加粗

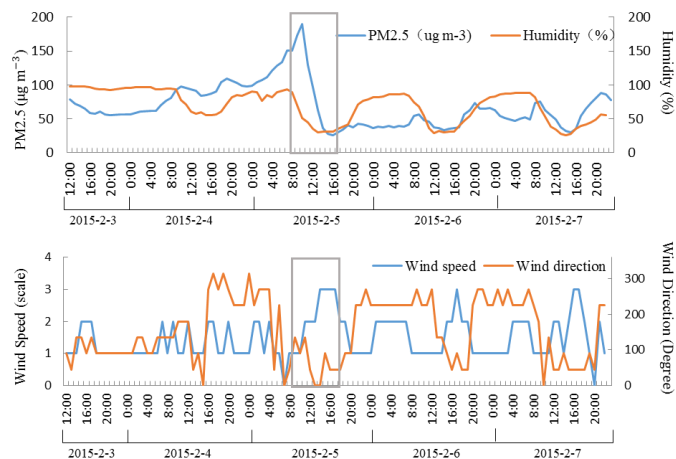


Figure 9. Surface PM_{2.5} concentrations, humidity, wind speed and wind direction measured by Lin'an regional background station (30°18' N, 119°44' E) on 3rd-7th February.

- 5 A dispersion process of PM_{2.5} was also recorded by sampling campaign on 5th February (see Figure 9). Particles was accumulating at BST 6:00 on 4th February and remained relative high concentration level (70-100 μg m⁻³). Then, PM_{2.5} concentrations started to enhance at BST 0:00 on 5th February and climbed to their peak value ~190 μg m⁻³ with the wind turning from south to northwest. Five hours later the PM_{2.5} concentration decreased sharply from 190 μg m⁻³ to 26 μg m⁻³. The pollution was diluted due to the clean southeast wind. The PM_{2.5} concentrations generally show a negative gradient in all
- 10 four flights, -0.123, -0.019, -0.013, and -0.010 for flight-1 (BST 8:08-8:45), -2 (BST 10:44-11:21), -3 (BST 14:14-14:52) and -4 (BST 15:25-15:59), respectively. The wind speed at each height level increased by more than 50% and the wind coming from northeast which led to the rapid reduction of PM_{2.5} at each height layer.

4 CONCLUSIONS

- 15 In this study, an UAV was customized for fine particulate matter research and thus flexibly equipped with portable commercial monitors. 3D images of PM_{2.5} were successfully mapped with high spatial resolution sampling data. Microscopic spatiotemporal patterns of PM_{2.5} concentration in eastern China are characterised in this research. 20 vertical profiles of PM_{2.5} concentrations were acquired revealing the diurnal variations of particle vertical distribution. Additionally, accumulation and dispersion events of PM_{2.5} pollution were successfully captured and detailedly discussed in the manuscript.

带格式的：字体：10 磅，非加粗

This study demonstrates the capability of UAVs to capture high spatial resolution data in atmosphere research. The major findings are listed as follows: (I) the distribution of PM_{2.5} concentrations presents obvious stratification phenomenon in morning flights while it becomes more homogenous in afternoon flights. PM_{2.5} concentration levels over 500 m height in afternoon flights are generally higher than those of morning flights (except for on February 5th, 2015). This indicates that the planetary boundary layer (PBL) height and inversion layers have a significant impact on the near ground PM_{2.5} concentration. (II) The vertical variations of PM_{2.5} concentration are bigger than the horizontal variations in terms of small scale space, although horizontal wind and hilly terrain could affect the horizontal distribution of PM_{2.5} concentrations. (III) PM_{2.5} concentrations are positively correlated with dew point temperature, which likely reflects the compound aerosol-cloud interactions. The high relative humidity is the major inducing factor for the heavy air pollution, especially in autumn and winter.

However, it is still challenging to monitor the evolution of atmosphere structure and fine particulate matter for a long time, considering the limitation of monitors' battery endurance and the UAV maximum payload. The potential of this flexible UAV platform will be further explored in future atmosphere research.

ACKNOWLEDGMENTS

The authors are grateful to Shanghai Environmental Protection Bureau, Shanghai Environmental Monitoring Center, Science Technology Department of Zhejiang Province (2014C31028), and the State Key Laboratory of Ocean Engineering of China at Shanghai Jiao Tong University for help with their support. The authors also express appreciation for the Second Surveying and Mapping Institute of Zhejiang Province for cooperation in manipulating the UAV for these experiments.

REFERENCES

- Altstalter, B., Platis, A., and Wehner, B.: ALADINA—an unmanned research aircraft for observing vertical and horizontal distributions of ultrafine particles within the atmospheric boundary layer, *Atmos. Meas. Tech.*, 8, 1627-1639, 2015.
- [Air Quality and Climate Change Research: https://www.epa.gov/air-research/air-quality-and-climate-change-research_2](https://www.epa.gov/air-research/air-quality-and-climate-change-research_2)
[March, 2014.](#)
- Bates, T. S., Quinn, P. K., Johnson, J. E., Corless, A., Brechtel, F. J., Stalin, S. E., Meinig, C., and Burkhardt, J. F.: Measurements of atmospheric aerosol vertical distributions above Svalbard, Norway, using unmanned aerial systems (UAS), *Atmos. Meas. Tech.*, 6, 2115–2120, 2013.
- [Booth, B. B., Dunstone, N. J., Halloran, P. R., Andrews, T., & Bellouin, N.: Aerosols implicated as a prime driver of twentieth-century North Atlantic climate variability, *Nat.*, 484, 7393, 2012.](#)

- Boy, M., Hellmuth, O., Korhonen, H., Nilsson, E. D., ReVelle, D., Turnipseed, A., Arnold, F., and Kulmala, M.: MALTE – model to predict new aerosol formation in the lower troposphere, *Atmos. Chem. Phys.*, 6, 4499–4517, doi:10.5194/acp-6-4499-2006, 2006.
- 5 [Brady, J. M., Stokes, M. D., Bonnardel, J., and Bertram, T. H., Characterization of a quadrotor unmanned aircraft system for aerosol-particle-concentration measurements, *Environ. Sci. Tech.*, 50, 1376-1383, doi:10.1021/acs.est.5b05320, 2016.](#)
- Cheung, H. C., Wang, T., and Baumann, K.: Influence of regional pollution outflow on the concentrations of fine particulate matter and visibility in the coastal area of southern China, *Atmos. Environ.*, 39, 6463-6474, 2005.
- Clarke, A. D., Ahlquist, N. C., Howell, S., and Moore, K.: A miniature optical particle counter for in situ aircraft aerosol research, *J. Atmos. Ocean. Tech.*, 19, 1557–1566, 2002.
- 10 Davidson, C. I., Phalen, R. F., and Solomon, P. A.: Airborne particulate matter and human health: a review, *Aerosol Sci. Technol.*, 39, 737-749, 2005.
- Day, D. E., Malm, [W. C.](#), and Kreidenweis, S. M.: Aerosol Light Scattering Measurements as a Function of Relative Humidity, *J. Air Waste Manage.*, 50, 710-716, 2000.
- 15 Ding, A., Wang, T., and Xue, [L., et al.](#): Transport of north China air pollution by midlatitude cyclones: Case study of aircraft measurements in summer, *J. Geophys. Res.*, 114, [D8](#), 2009.
- Ding, G. A., Chen, Z. Y., and Gao, Z. Q.: Vertical Distribution and Its Dynamic Characteristics of PM_{2.5} and PM₁₀ in Lower Atmosphere in Beijing, *Sci. China, Ser. D*, 35, 31-44, 2005.
- Dominici, F., Peng, R. D., Bell, M. L., Pham, L., McDermott, A., Zeger, S. L., and Samet, J. M.: Fine particulate air pollution and hospital admission for cardiovascular and respiratory diseases, *J. Am. Med. Assoc.*, 295, 1127-1134, 2006.
- 20 Harnisch, F., Gohm, A., Fix, A., Schnitzhofer, R., Hansel, A., and Neisinger, B.: Spatial distribution of aerosols in the Inn Valley atmosphere during wintertime, *Meteorol. Atmos. Phys.*, 103, 1, 223–235, 2009.
- [Quan, J., Zhang, Q., He, H., and Liu, J.: Analysis of the formation of fog and haze in North China Plain \(NCP\), *Atmos. Chem. Phys.*, 11, 8205-8214, 2011.](#)
- 25 Illingworth, S. M., Allen, G., Percival, C., Hollingsworth, P., Gallagher, M. W., Ricketts, R., Hayes, H., Ladosz, P., Crawley, D., and Roberts, G.: Measurement of boundary layer ozone concentrations on-board a Skywalker Unmanned Aerial Vehicle, *Atmos. Sci. Lett.*, 15, 4, 252–258, doi:10.1002/asl2.496, 2014.
- [Li, J., Fu, Q., Huo, J., Wang, D., Yang, W., Bian, Q., et al.: Tethered balloon-based black carbon profiles within the lower troposphere of Shanghai in the 2013 East China smog, *Atmos. Environ.*, 327-338, 2015.](#)
- 30 Liao, X., Zhang, X., and Wang, Y.: Comparative Analysis on Meteorological Condition for Persistent Haze Cases in Summer and Winter in Beijing. *Environ. Sci.*, 35, 2031-2044, 2014.
- Maletto, A., McKendry, I. G., and Strawbridge, K. B.: Profiles of particulate matter size distributions using a balloon-borne lightweight aerosol spectrometer in the planetary boundary layer, *Atmos. Environ.*, 37, 661-670, 2003.

- Mamouri, R. E., Nisantzi, A., Hadjimitsis, D. G., Ansmann, A., Schwarz, A., Sasart, S., and Baldasano, J. M.: Complex vertical layering and mixing of aerosols over the eastern Mediterranean: active and passive remote sensing at the Cyprus University of Technology. In First International Conference on Remote Sensing and Geoinformation of Environment, Int. Soc. Opt. Photon, 879517, [doi:10.1117/12.2028426](https://doi.org/10.1117/12.2028426), 2013.
- 5 [Meng, Z., Jia, X., Zhang, R., Yu, X., and Ma, Q.: Characteristics of PM_{2.5} at Lin'an Regional Background Station in the Yangtze River Delta Region. *J. Appl. Meteorol. Sci.*, 23, 424-432, 2012.](#)
- McKendry, I. G., Sturman, A. P., [and](#) Vergeiner, J.: Vertical profiles of particulate matter size distributions during winter domestic burning in Christchurch, New Zealand, *Atmos. Environ.*, 38, 4805-4813, 2004.
- Ouyang, Y.: China wakes up to the crisis of air pollution, *Lancet Respir. Med.*, 1, 12, 2013.
- 10 [Padr6-Martinez, L. T., Patton, A. P., Trull, J. B., Zamore, W., Brugge, D., and Durant, J. L.: Mobile monitoring of particle number concentration and other traffic-related air pollutants in a near-highway neighborhood over the course of a year, *Atmos. Environ.*, 61, 253-264, 2012.](#)
- Peng, Z. R., Wang, D., Wang, Z., Gao, Y., [and](#) Lu, S.: A study of vertical distribution patterns of PM_{2.5} concentrations based on ambient monitoring with unmanned aerial vehicles: a case in Hangzhou, China, *Atmos. Environ.*, 123, 357-369, [doi:10.1016/j.atmosenv.2015.10.074](https://doi.org/10.1016/j.atmosenv.2015.10.074), 2015.
- 15 [Platis, A., Altstalter, B., Wehner, B., Wildmann, N., Lampert, A., and Hermann, M., et al.: An observational case study on the influence of atmospheric boundary-layer dynamics on new particle formation. *Boundary-Layer Meteorol.*, 158, 1, 1-26, 2015.](#)
- Pope, C. A., Burnett, R. T., Krewski, D., Jerrett, M., and Shi, Y.: Cardiovascular mortality and exposure to airborne fine particulate matter and cigarette smoke shape of the exposure-response relationship, *Circ.*, 120, 941-948, 2009.
- 20 Pope, C. A., Burnett, R. T., Thun, M. J., Calle, E. E., Krewski, D., Ito, K., and Thurston, G. D.: Lung cancer, cardiopulmonary mortality, and long-term exposure to fine particulate air pollution, *J. Am. Med. Assoc.*, 287, 1132-1141, 2002.
- Ramana, M., Ramanathan, V., Kim, D., Roberts, G. C. and Corrigan, C. E.: Albedo, atmospheric solar absorption and heating rate measurements with stacked UAVs, *Q. J. Meteorol. Soc.*, 133, 1913-1931, 2007.
- 25 Ramanathan, V., Ramana, [M. V.](#), Roberts, [G.](#), Kim, [D.](#), Corrigan, [C.](#), Chung, [C.](#), and Winker [D.](#): Warming trends in Asia amplified by brown cloud solar absorption, *Nat.*, 448, 575-578, 2007.
- [Ramachandran, G., Adgate, J. L., Pratt, G. C., and Sexton, K.: Characterizing Indoor and Outdoor 15 Minute Average PM_{2.5} Concentrations in Urban Neighborhoods. *Aerosol Sci. Technol.*, 37, 1, 33-45, \[doi: 10.1080/02786820300889\]\(https://doi.org/10.1080/02786820300889\), 2003.](#)
- 30 [Renard, J. B., Dulac, F., Berthet, G., Lurton, T., Vignelles, D., et al.: LOAC: a small aerosol optical counter/sizer for ground-based and balloon measurements of the size distribution and nature of atmospheric particles – Part 2: First results from balloon and unmanned aerial vehicle flights, *Atmos. Meas. Tech. Disc.* 8, 1261-1299, 2016.](#)
- Šmil, V., and Hofman, R.: Tracking of atmospheric release of pollution using unmanned aerial vehicles, *Atmos. Environ.*, 67, 425-436, 2013.

[Stevens, B., and Boucher, O.: Climate science: The aerosol effect. Nat. 40-41, 2012.](#)

Strawbridge, K. B., and Snyder, B. J.: Daytime and nighttime aircraft lidar measurements showing evidence of particulate matter transport into the northeastern valleys of the Lower Fraser Valley, BC, Atmos. Environ, 38, 5873-5886, 2004.

5 Thomas, R. M., Lehmann, K., Nguyen, H., Jackson, D. L., Wolfe, D., and Ramanathan, V.: Measurement of turbulent water vapor fluxes using a lightweight unmanned aerial vehicle system, Atmos. Meas. Tech., 5, 243–257, doi:10.5194/amt-5-243-2012, 2012.

Van den Kroonenberg, A., Martin, T., Buschmann, M., Bange, J., and Vörsmann, P.: Measuring the wind vector using the autonomous mini aerial vehicle M2AV, J. Atmos. Ocean. Tech., 25, 1969–1982, 2008.

10 Wang, W., Ma, J., and Hatakeyama, S.: Aircraft measurements of vertical ultrafine particles profiles over Northern China coastal areas during dust storms in 2006, Atmos. Environ., 42, 5715-5720, 2008.

[Wang, Z., Lu, F., He, H., Lu, Q., Wang, D., and Peng, Z. R.: Fine-scale estimation of carbon monoxide and fine particulate matter concentrations in proximity to a road intersection by using wavelet neural network with generic algorithm. Atmos. Environ, 104, 264-272, 2015.](#)

15 [Wang, Z., Lu, Q. C., He, H. D., Wang, D., Gao, Y., and Peng, Z. R.: Investigation of the spatiotemporal variation and influencing factors on fine particulate matter and carbon monoxide concentrations near a road intersection. Frontiers of Earth Science, 1-13: Investigation of the spatiotemporal variation and influencing factors on fine particulate matter and carbon monoxide concentrations near a road intersection. Front. Earth Sci., doi:10.1007/s11707-016-0564-5, 2016.](#)

[Wang, Z., He, H., Lu, F., Lu, Q., and Peng, Z.: Hybrid model for prediction of carbon monoxide and fine particulate matter concentrations near road intersection. Transp. Res. Rec.: J. Transp. Res. Bd. 2503, 29-38, 2015.](#)

20 Wildmann, N., Kaufmann, F., and Bange, J.: An inverse modelling approach for frequency response correction of capacitive humidity sensors in ABL research with small unmanned aircraft, Atmos. Meas. Tech., 7, 4407–4438, doi:10.5194/amtd-7-4407-2014, 2014a.

Wildmann, N., Hofstätter, M., Weimer, F., Joos, A., and Bange, J.: MASC—a small remotely piloted aircraft (RPA) for wind energy research, Adv. Sci. Res., 11, 55–61, doi:10.5194/asr-11-55-2014, 2014b.

25 Wildmann, N., Mauz, M., and Bange, J.: Two fast temperature sensors for probing of the atmospheric boundary layer using small remotely piloted aircraft (RPA), Atmos. Meas. Tech., 6, 8, 2101–2113, doi:10.5194/amt-6-2101-2013, 2013.

Zhang, J., Zhang, S. J., Zhu, Z. Y., Zhang, Y. F., and Ya-Qin, J. I.: Numerical simulation of the optimal placement of aerosol sampling-head on an unmanned aerial vehicle, China Environ. Sci., 34, 9, 2192-2198, 2014.